

Effect of Gas-solid Thermal Coupling on Loading Capacity of Aerostatic Bearing under Micro-scale Gas-film

Hui Chai^{1,a}, Caiqi Li^{2,b}, Wei Long^{1,c}

¹Faculty of Mechanical and Electrical Engineering, Kunming University of Science and Technology, Kunming, China

²School of Materials Science and Engineering, Kunming University of Science and Technology, Kunming, China

^ahenry0806@126.com, ^blcq137211@126.com, ^c28775248@qq.com

Keywords: aerostatic bearing; micro-scale gas film; gas-solid thermal coupling; loading characteristics

Abstract: When the aerostatic bearing working gas film is at the micron-scale, the pressure distribution in the gas film has a significant temperature sensitivity, which seriously affects the loading capacity and stiffness characteristics of the bearings system. Based on the theory of gas lubrication and rarefied gas dynamics, combined with boundary slip and gas-solid thermal coupling analysis technology, this paper studies the local deformation of aerostatic bearing caused by temperature influence by numerical analysis method, and theoretically analyses and experimentally studies the loading capacity and stiffness characteristics of the bearing system.

1. Introduction

Aerostatic bearings with high precision, low friction power consumption and non-polluting advantages, are widely used in high-precision testing equipment, ultra-precision machining machine tools and aircraft flight testing and other fields^[1]. Along with the changing working environment, all kinds of precision instruments are more and more demanding on the reliability and working stability of bearing, not only to ensure the normal work in the range of (-250~315) °C, but also to ensure the stability of the spindle during the rotation and the bearing seat, and to relieve the impact and vibration between them. On the macroscopic scale, based on the isothermal assumption, ignoring the temperature change can satisfy the work requirement. However, with the decreasing of the gas film thickness and the continuous improvement of the precision, the flow form of the gas film in the micro-scale will present the transition from the layer to the slip flow^[2].

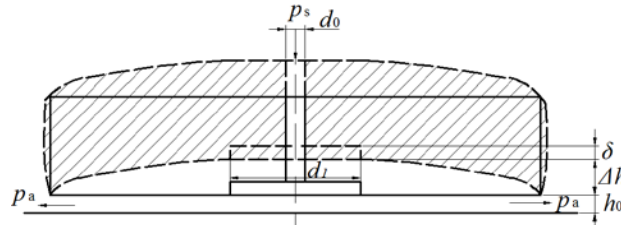
Domestic scholars on the loading characteristics of aerostatic bearings mostly from GUO^[3], LONG^[4] from the negative damping angle and fluid lubrication theory, the change of aerostatic bearing structure parameters and operating parameters to analyze the bearing vibration characteristics and loading characteristics of the impact. YS Chen^[5] has studied the stiffness of various geometric designs of aerostatic journal bearings under different gas supply pressures, and the stiffness characteristics of the aerostatic bearings is evaluated experimentally. For the first time, DJ Chen^[6] introduced the rarefaction flow factor into the Reynolds equation. The finite element difference method was used to study the loading capacity and stiffness of the bearing through Matlab software.

Although the existing research has done a lot of analysis on the loading capacity and stiffness of aerostatic bearings, but ignores the influence of temperature on micro-structure characteristics inside gas film of aerostatic bearing, This not only affects the shape and thickness of the lubricating gas film, but also further changes the loading capacity and stiffness of the aerostatic bearing through the gas-solid thermal coupling method. The result of numerical analysis has a large deviation from the experimental results, which seriously affects and restricts the calculation reliability of the aerostatic bearing in the micron scale. Therefore, it is necessary to further study the temperature

sensitivity of the aerostatic bearing gas film at the micro-scale. Finally, the experimental and numerical results are compared and verified, which will play a guiding role in improving the machining accuracy of high precision instruments.

2. Working principle and mathematical model

The aerostatic bearing provides the high pressure gas source through the gas compressor, the gas film is introduced through the throttle hole, and the loading capacity is borne through the gas film formed in the clearance of the bearing. In this paper, the disc type central gas supply small hole throttle static thrust bearing with a diameter of $D=50$ mm is selected as the research object. Bearing structure schematic diagram as shown in Fig. 1 solid line outline, gas hole diameter $d_0=0.2$ mm, gas cavity depth $\delta=0.2$ mm, gas cavity diameter $d_1=3$ mm.



P_s - the gas pressure of the throttle hole, Δh - the deformation of the gas film, h_0 - the support of average thickness of gas film, P_a - atmospheric pressure

Fig.1 Deformation of gas film with bidirectional gas-solid coupling in aerostatic bearing

Under the condition of normal temperature, the effect of thermal coupling and velocity slip is not considered. Based on the principle of aerostatic lubrication, the motion law of the flow field in the gas film can be expressed as Navier-Stokes (N-S) equation.

The momentum equation in the X direction:

$$\frac{\partial p}{\partial x} = \mu \frac{\partial^2 u}{\partial y^2} \quad (1)$$

The momentum equation in the Z direction:

$$\frac{\partial p}{\partial z} = 0 \quad (2)$$

The momentum equation in the Y direction:

$$\frac{\partial p}{\partial y} = \mu \frac{\partial^2 w}{\partial y^2} \quad (3)$$

Gas State equation:

$$p = \rho RT \quad (4)$$

Continuity equation:

$$\frac{\partial(\rho u)}{\partial x} + \frac{\partial(\rho v)}{\partial y} + \frac{\partial(\rho w)}{\partial z} + \frac{\partial \rho}{\partial t} = 0 \quad (5)$$

In the form: ρ - gas density, μ - dynamic viscosity of gas, p - gas pressure, u , v , w - velocity component in x , y , z direction, T - temperature.

However, when the gas film thickness of the aerostatic bearing is in the micron-scale or even below, due to the small scale of the fluid characteristic, the Kn number will increase, which makes the gas at the micro-scale have the same characteristics as the rarefied gas. The flow pattern of supporting gas film is in the transition stage of slip flow or laminar flow slip flow. The traditional N-S equation will not well reflect the characteristics of boundary slip flow and pressure distribution. No slip boundary conditions will no longer apply to micro-scale flow analysis. Based on the influence of the boundary slip on the [7] and the gas stratification theory [16], the velocity slip

boundary conditions need to be supplemented at this time:

$$z = 0 \text{ 时}, \quad u = U + l' \frac{\partial u}{\partial z} \quad v = l' \frac{\partial w}{\partial z} \quad w = 0 \quad (6)$$

$$z = h \text{ 时}, \quad u = -l' \frac{\partial u}{\partial z} \quad v = -l' \frac{\partial w}{\partial z} \quad w = u \frac{\partial h}{\partial x} + v \frac{\partial h}{\partial y} \quad (7)$$

The above formula (1), (2), (3) is brought into the formula (6), (7) to solve the u , v , w and into the formula (4), (5) the micro-scale of the Reynolds equation can be simplified as:

$$\begin{aligned} & \frac{\partial}{\partial x} \left(ph^3 \frac{\partial p}{\partial x} \right) + \frac{\partial}{\partial y} \left(ph^3 \frac{\partial p}{\partial y} \right) \\ & = \frac{6\mu U}{1 + 6k'_n} \frac{\partial(ph)}{\partial x} + \frac{12\mu}{1 + 6k'_n} \frac{\partial(ph)}{\partial t} \end{aligned} \quad (8)$$

In the form: $k'_n = \frac{2 - \sigma_v}{\sigma_v}$; σ_v - molecular tangential momentum adjustment coefficient.

In actual work, with the increase of ambient temperature and bearing local temperature, the uneven thermal deformation of the bearing in height direction and the expansion of gas inside the gas film lead to the change of the flow field inside the flat supporting gas film, as shown in Fig. 1, the outline of the dashed line. At this time, the gas film is deformed in the vertical height direction, and the deformation amount is Δh . The deformation of the edge of the gas cavity is the largest. It is recorded as Δh_{\max} and is nonlinear decreasing to the radius direction. The change of gas film thickness can be expressed by the formula as follows.

$$\begin{aligned} h &= \begin{cases} h_0 + \Delta h + \delta_i \delta, r = \left(0, \frac{d_1}{2} \right) \\ h_0 + \Delta h, r > d_1 \end{cases} \\ \delta_i &= \begin{cases} 1, \sqrt{x^2 + y^2} < \frac{d_1}{2} \\ 0, \frac{d_1}{2} < \sqrt{x^2 + y^2} < \frac{D}{2} \end{cases} \end{aligned} \quad (9)$$

In the form: P - the pressure of gas supply, h - the effective gas film thickness, h_0 - the support of average thickness of gas film, δ_i - Kronecker delta, η - the viscosity of gas after pressurization, u , v - the velocity of x , y in the gas film, respectively, r - distance along the flow direction.

The formula (9) is brought into the formula (8), and the formula of Reynolds equation after the gas film deformation is obtained.

$$\begin{aligned} & \frac{\partial}{\partial x} \left(p(h_0 + \Delta h)^3 \frac{\partial p}{\partial x} \right) + \frac{\partial}{\partial y} \left(p(h_0 + \Delta h)^3 \frac{\partial p}{\partial y} \right) = \\ & \frac{6\mu U}{1 + 6k'_n} \frac{\partial(p(h_0 + \Delta h))}{\partial x} + \frac{12\mu}{1 + 6k'_n} \frac{\partial(p(h_0 + \Delta h))}{\partial t} \end{aligned} \quad (10)$$

3. Temperature sensitivity of gas film

3.1 Numerical analysis

In this paper, a two-way fluid solid coupling model of pinhole throttling aerostatic bearing is established. The Fluent and Static Structural modules in Ansys Workbench are used to initialize the fluid domain and solid domain respectively. The setting mainly includes the boundary condition, the gas-solid coupling surface, the solution model and the monitoring setting, and the convective temperature should be set in the boundary condition. It needs special description that in the Static Structural module, the three-dimensional flow field and pressure distribution in the micro gas film gap of the Fluent module can be coupled to the aerostatic bearing in the solid domain, and then the

small deformation of the aerostatic bearing under certain working conditions can be obtained. The large eddy simulation (LES) should be used in the analysis of the fluid domain model, because it can better calculate the flow characteristics and pressure distribution of gas in the gas film. The grid distortion is 0.05, which satisfies the calculation precision. The bearing material is aluminum alloy, and the pressure distribution inside the gas film is coupled to temperature. The maximum deformation Δh_{\max} of the gas film height direction is obtained, and the variation rule shown in Fig. 2 and Fig. 3 is obtained.

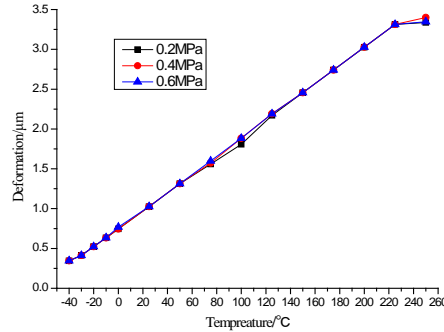


Fig.2 The maximum deformation Δh_{\max} of $5\mu\text{m}$ gas film under different gas supply pressures

As shown in Fig. 2, as the temperature increases, the deformation of the gas film increases linearly. When the temperature reaches about 250°C , the deformation tends to be stable. This may be due to the thermal deformation of the aerostatic bearing and the thermal expansion of the gas in the gas film as the temperature increases. The gas film is deformed by the deformation of the gas film, and because the center of the gas film is a gas high pressure region, the deformation of the gas film is maximum at the edge of the gas cavity, and the deformation amount in the radial direction inside the gas film gradually decreases.

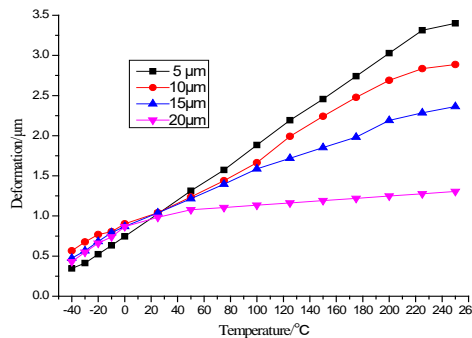


Fig.3 The maximum deformation Δh_{\max} of different gas film thickness under $p_s=0.4\text{MPa}$

As shown in Fig. 3, as the temperature increases, the gas film deformation overall increases, but the slope decreases with the increase of the gas film thickness. Before 25°C , the corresponding deformation of $5\mu\text{m}$ gas film is the smallest, and the deformation of $(10\sim 20)\mu\text{m}$ gas film is very different. After 25°C , with the increase of gas film thickness, the corresponding deformation of $5\mu\text{m}$ gas film rapidly increased, and the deformation of $(10\sim 20)\mu\text{m}$ gas film began to widen. The bigger the gas film thickness, the smaller the deformation. Especially at 25°C , when the gas film thickness is $(5\sim 20)\mu\text{m}$, the maximum deformation Δh_{\max} of the gas film is maintained at about $1\mu\text{m}$.

It is necessary to point out that when the gas film thickness is $20\mu\text{m}$, the deformation amount is between $(1\sim 1.5)\mu\text{m}$ with the increase of temperature. This is mainly because the gas film is in a fully developed laminar state when the gas film thickness is $20\mu\text{m}$ or above. The sensitivity of the gas film to temperature is reduced. The internal flow can be described by the traditional N-S equation. At that time, the sensitivity of the gas film to temperature is very low. Therefore, the maximum deformation Δh_{\max} is lower than that of other gas film thickness. In contrast, when the gas film thickness is reduced to $5\mu\text{m}$ or below, by the gas stratification theory, slip zone proportion increases, resulting in the N-S equation and the laminar flow hypothesis is not the traditional well reflect the internal flow characteristics. So it is necessary to use the thin layer flow velocity slip

conditions, the gas film in large deformation in the range of temperature increase linearly. The flow state and pressure distribution of the gas film shows the work inside will have a temperature sensitive characteristic strongly, the flow characteristics and pressure distribution in the gas film will change, which will affect the stiffness and loading capacity of the system.

Based on this, the large eddy simulation (LES) model is applied to calculate the pressure distribution inside the unsteady gas film considering the thermal coupling effect of temperature, and the effect of temperature and thermal coupling on the loading capacity and stiffness of the inner gas film of aerostatic bearing is verified by experiments. The pressure distribution shown below is shown in Fig. 4.

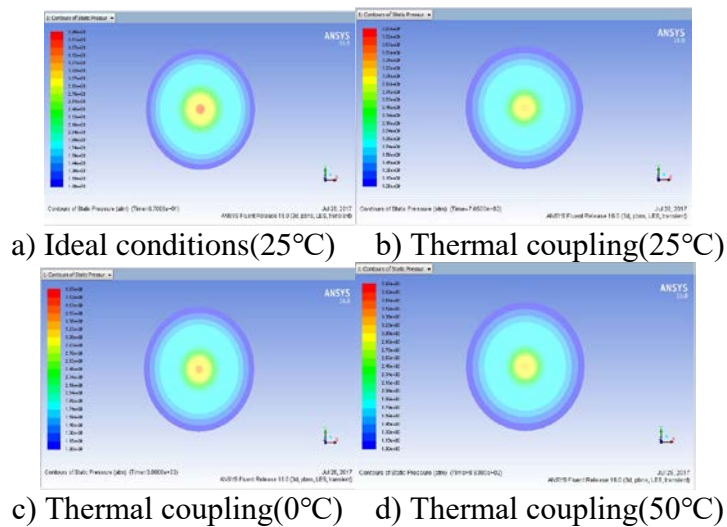
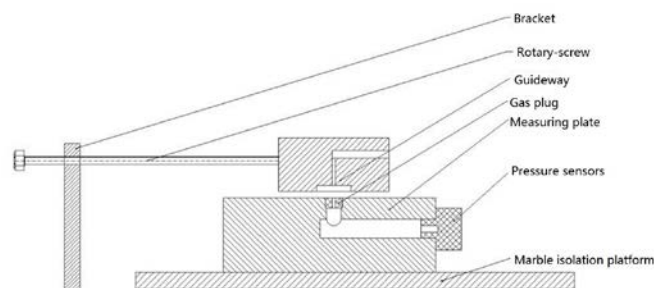


Fig.4 Pressure distribution figure under different temperature conditions

Fig.4-a) and Fig.4-b) shows, when 25°C under ideal conditions and considering the thermal coupling condition, the gas film center showed a redundant high-pressure gas zone, but considering the thermal coupling calculation of high pressure area of the center becomes small, basically reached the high level 0.38MPa under ideal conditions. As shown in Fig. 4-c), 4-b) and 4-d), considering the thermal coupling condition, with the increase of the temperature in the range of 0~50°C, the range of the central high pressure area of the gas film decreases gradually, and the maximum pressure value can be reduced from 0.38MPa to 0.29MPa. It can be seen that gas-solid thermal coupling will cause some deformation of aerostatic bearing in the direction of gas film height, especially for small gas film ($\leq 5\mu\text{m}$) will cause greater deformation, which will seriously affect the pressure distribution inside the gas film and the maximum pressure value in the high pressure area. Moreover, the coupling effect is very sensitive to temperature. With the increase of temperature, the sensitivity of gas film increases rapidly, which will further affect the stiffness of gas film and restrict its loading capacity of the aerostatic bearing.

3.2 Experimental verification



a) Operational principle figure



b) Experimental installation figure

Fig.5 Gas film pressure test equipment

According to the working principle, we set up the experimental device as shown in Fig. 5, the outer diameter of the disc aerostatic bearing is $D=50\text{mm}$, gas hole diameter $d_0=0.2\text{ mm}$, gas cavity depth $\delta=0.2\text{ mm}$, gas cavity diameter $d_1=3\text{ mm}$. the pressure sensor (BSHA-1) range is 50kg, and the output sensitivity 30~50mv/v. During the experiment, 800 sets of data were measured accumulatively. Each group of data was measured repeatedly after three times, and the average value was obtained, and the pressure distribution diagram, as shown in Fig. 6, was obtained.

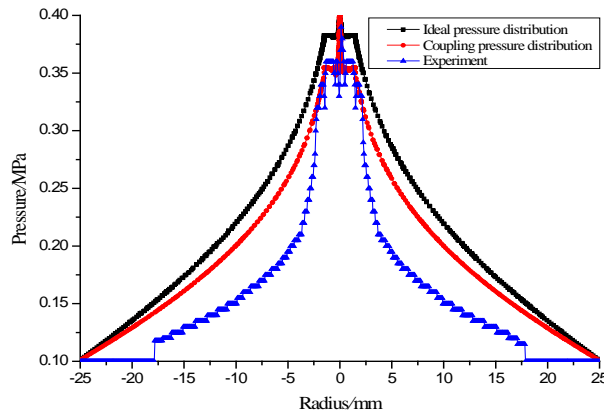


Fig.6 $h=10\mu\text{m}, p_s=0.4\text{MPa}$ in the radial direction of the gas film pressure distribution

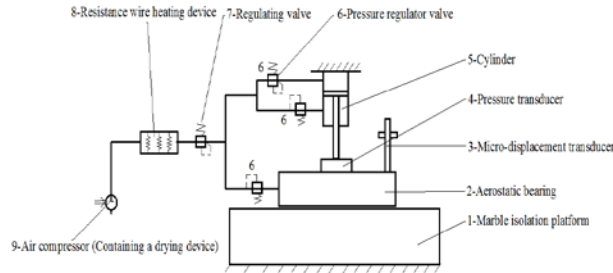
As shown in Fig. 6, the internal pressure distribution along the radius direction of the gas film is gradually decreased, the calculated pressure distribution in high pressure area of the experiment is consistent with coupling simulation, high pressure area can reach (0.35~0.37)MPa, The experimental pressure distribution has a great error compared with the ideal pressure distribution, and the ideal pressure distribution is significantly higher than that of the thermal coupling and experimental pressure distribution. It can be seen that if the loading capacity of the coupling is not considered only under the ideal numerical analysis condition, the overload is easily caused in the actual working process. The results of numerical calculation of gas-solid thermal coupling can be better consistent with the experiment and more practical. The gas pressure measured near the periphery of the aerostatic bearing is basically fixed to 0.1MPa along the radial direction, which is mainly due to the difficulty of measuring the accuracy of the experimental equipment in the periphery. The obvious pressure drop is observed in the thermal coupling and experimental pressure distribution, and it can be obtained that gas vortex is generated near the gas cavity, this lays the foundation for the follow-up study of aerostatic bearing in consideration of the gas vortex and micro-vibration under the condition of gas-solid thermal coupling.

4. Influence of gas-solid thermal coupling on loading capacity of aerostatic bearing

4.1 Experimental design

The principle and device of the experiment are shown in Fig.7. In the experiment, the

temperature is measured by a standard glass mercury thermometer. The range of measurement is $(-30\sim 300)^{\circ}\text{C}$ and the fraction is 0.1°C . Dry ice creates a low temperature environment, and all the measurement processes are instantaneous. By measuring the loading capacity of the bearing under different gas film thickness and temperature conditions, the variation rule of the loading characteristics of aerostatic bearing considering the gas-solid thermal coupling and ideal condition is compared and analyzed by the experimental data.



a) Experimental schematic diagram

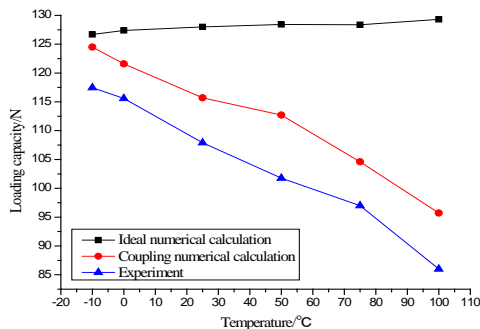


b) Experimental graph

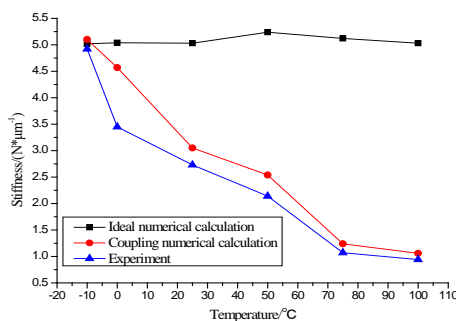
Fig.7 Schematic diagram and test equipment for bearing capacity of solid-heat coupling

4.2 Interpretation of result

The results of the experimental and numerical analysis of the loading characteristics of the aerostatic bearing are compared with the results of the following results.



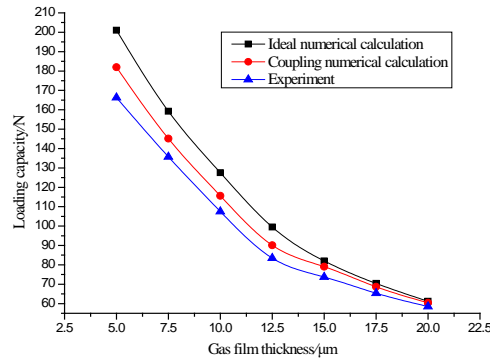
a) Change curve of loading capacity



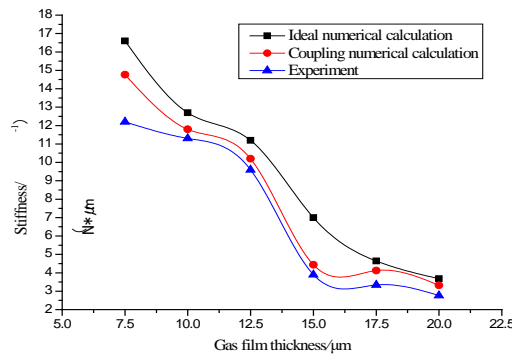
b) Change curve of stiffness

Fig.8 Different temperature conditions loading capacity under $10\mu\text{m}, p_s=0.4\text{MPa}$

As shown in Fig. 8, the ideal numerical calculation results, with the increase of temperature, loading capacity of the aerostatic bearing and stiffness of the gas film occurs slight fluctuations and the difference is small. But the experimental results with the increasing of temperature, the loading capacity and stiffness decreased. At the same time considering the observation of gas-solid thermal coupling, with the increase of temperature, loading capacity of the aerostatic bearing and stiffness of the gas film is gradually reduced. Neglecting the influence of the error factors in the experiment, the variation of the experimental data is more close to the numerical results of the gas-solid thermal coupling. This is mainly due to the expansion of gas in the gas film due to the increase of temperature. The distance between gas molecules increases, and the number of gas molecules in the unit volume decreases, which leads to the decrease of loading capacity of the aerostatic bearing and stiffness of the gas film.



a) Change curve of loading capacity



b) Change curve of stiffness

Fig.9 Different gas film thickness loading capacity under $25^{\circ}\text{C}, p_s = 0.4\text{MPa}$

As shown in Fig. 9, in 25°C , the loading capacity and stiffness decreases with the increase of gas film thickness ($5\sim 20$) μm of aerostatic bearing, but the decline gradually reduced, which is mainly due to the sensitivity to temperature decreases with gas film thickness increasing, the influence on the loading capacity of the aerostatic bearing and stiffness of the gas film gradually reduced. In the ideal numerical results, loading capacity of the aerostatic bearing and stiffness of the gas film is gradually decrease with the increase of gas film thickness ($5\sim 20$) μm . The experimental results show that the loading capacity and stiffness decrease with the increase of the gas film thickness, but the numerical value is quite different from the ideal numerical calculation. The numerical value is more close to the experimental data under the coupling condition. It should be noted that the gas film stiffness decreases rapidly with the increase of gas film thickness at ($12.5\sim 20$) μm .

This is mainly because with the increase of the gas film thickness, gas flow characteristic from the rarefied flow gradually transition to steady laminar flow, the gas molecules are driven by viscous force along the radius direction to realize the smooth motion, and the interaction between the vertical direction of the molecular layer decreased, thus weakening the bearing height direction of gas film stiffness. Ignoring the influence of system errors in experiment, it is obvious that the experimental data are more consistent with the numerical calculation considering gas-solid thermal coupling, which is quite different from the traditional numerical analysis under isothermal condition

without considering gas-solid thermal coupling. Therefore, when designing and analyzing aerostatic bearing under wide range of temperature changes, we must give full consideration to the effect of thermal coupling effect of gas-solid two phase on the performance of bearing, and the conclusion is of practical significance.

5. Conclusion

(1) With the increase of temperature, the total deformation of gas film increases linearly. When the temperature reaches 250°C, the deformation tends to be stable. But with the increase of gas supply pressure, the deformation of gas film has small difference. With the increase of temperature, gas film deformation increased. But with the increase of gas film thickness the slope of the curve decreases, the temperature sensitivity of the gas film decreases gradually.

(2) By comparing the ideal and the gas-solid thermal coupling under the condition of high-pressure zone, gas-solid thermal coupling will cause the aerostatic bearing deformation occurs in the height direction of the gas film, especially will cause greater deformation for the micro-scale gas-film ($\leq 5\mu\text{m}$), and seriously influence the gas film pressure distribution. And the coupling effect has very sensitive strong on the temperature, which will further affect the stiffness of gas film and restraint of loading capacity of aerostatic bearing.

(3) Through two groups of experiments, if only by numerical analysis under ideal conditions, calculation of loading capacity is too large to get experimental data, easy to cause the bearing overload. On the contrary, calculation of gas-solid thermal coupling results in better agreement with experiment, and the error is less than 8%. Considering the coupling effect of the pressure distribution calculation results and the measured pressure distribution the same trend, there is obvious pressure sharp drop.

Acknowledgment

Thank you very much for the project funded by the National Natural Science Foundation of China (No. 51766006). Thanks to Cai-qi LI and Wei LONG for their theoretical support. Corresponding Author: Hui CHAI, male, 1993, Master degree. Main research direction: fluid transmission and control. E-mail: henry0806@126.com.

References

- [1] ZHU Jincheng. Dynamic Characteristics and Nano-vibration of Aerostatic Bearings [D]. Wu Han: Huazhong University of Science and Technology, 2014.
- [2] ZHANG Haijun, ZHU Changsheng, Yangqin. Analysis of Rarefaction Effect on Steady Characteristic of Micro-gas Lubrication Journal Bearings [J]. Journal of Vibration and Shock, 2008, 27(S): 19-22.
- [3] GUO Liangbin, WANG Zuwen. New Method of Dynamic Test for Static Stiffness of Externally Pressurized Gas Bearing [J]. Chinese Journal of Mechanical Engineering, 2007, 43(4):21-26.
- [4] LONG Wei. Study on Loading Characteristics of Orifice Compensated Aerostatic Thrust Bearing [D]. Harbin Institute of Technology, 2010.
- [5] YS Chen, CC Chiu, YD Cheng. Influences of operational conditions and geometric parameters on the stiffness of aerostatic journal bearings [J]. Precision Engineering; 2010, 34(4):722-734.
- [6] CHEN Dongju ZHOU Shuai YANG Zhi et al. Influence of Flow Factor in Gas Rarefied Effects to Aerostatic Thrust Bearing Performance [J].Journal of Sichuan University (Engineering Science Edition), 2016, 48(1):194-199.
- [7] ZHANG Haijun, ZHU Changsheng, YANG Qin et al. Generalized maxwell velocity slip boundary model [J]. Scientia Sinica Physica, Mechanica & Astronomica, 2013(5):662-669.
- [8] NING Fangwei, LONG Wei, LIU Yan. Analysis of Gas Flow Mechanism and Pressure Characteristics between Plates in Micro Scale [J]. China Mechanical Engineering, 2016, 27(14):1862-1865.